



TITLE:

Phase Diagram of  $(M[x]M[x])$  Se ( $0 \leq x \leq 1$ ) ( $M, M' = 3d$ -transition metal) (Commemoration Issue Dedicated to Professor Toshio TAKADA On the Occasion of His Retirement)

AUTHOR(S):

Hayashi, Akihiko; Imada, Katsuhiro; Inoue, Kazumichi; Ueda, Yutaka; Kosuge, Koji

---

CITATION:

Hayashi, Akihiko ...[et al.], Phase Diagram of  $(M[x]M[x])$  Se ( $0 \leq x \leq 1$ ) ( $M, M' = 3d$ -transition metal) (Commemoration Issue Dedicated to Professor Toshio TAKADA On the Occasion of His Retirement). Bulletin of the Institute for Chemical Research, ...

ISSUE DATE:

1986-12-06

URL:

<http://hdl.handle.net/2433/77161>

RIGHT:

## Phase Diagram of $(M'_x M_{1-x})_3 \text{Se}_4$ ( $0 \leq x \leq 1$ ) ( $M, M' = 3d\text{-transition metal}$ )

Akihiko HAYASHI\*, Katsuhiro IMADA\*, Kazumichi INOUE\*,  
Yutaka UEDA\* and Koji KOSUGE\*

Received May 19, 1986

The phase diagram of  $(M'_x M_{1-x})_3 \text{Se}_4$  ( $0 \leq x \leq 1$ ;  $M, M' = 3d\text{-transition metal}$ ) was determined by DTA and high-temperature X-ray diffraction. The obtained phase diagrams were classified into two groups: (a) solid solution type; (b) phase separation type. In the (a) group, the phase transition from the  $\text{Cr}_3\text{S}_4$ - to  $\text{CdI}_2$ -structure was observed over a whole composition range in each system. In the (b) group, a solid solution with the  $\text{CdI}_2$ -structure was also observed at higher temperature. Some features of the phase diagram were discussed from the viewpoint of the cation distribution in these systems.

KEY WORDS: Phase diagram/ Transition metal chalcogenide/ Order-disorder transition/

### INTRODUCTION

The 3d-transition metal chalcogenides,  $M_{1+y}X_2$  ( $M$ : 3d-transition metal,  $X$ : chalcogen,  $0 \leq y \leq 1$ ), are of interest with respect not only to their various physical properties but also to the phase relation and structural aspect. A number of vacancy-ordered phases with the characteristic structures based on the  $\text{NiAs}$ - or  $\text{CdI}_2$ -structure,  $M_5X_8$ ,  $M_2X_3$ ,  $M_3X_4$ ,  $M_7X_8$  etc., appear in the composition range  $0 \leq y$

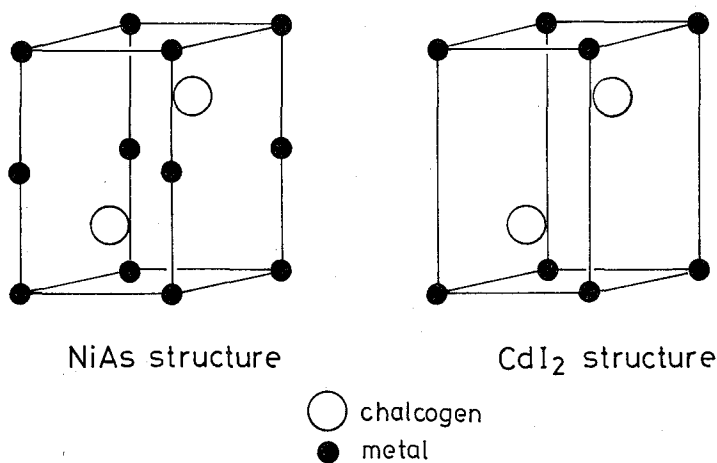


Fig. 1. Schematic drawing of the  $\text{NiAs}$ - and  $\text{CdI}_2$ -structure

\* 林 昭彦, 今田勝大, 井上和路, 上田 寛, 小菅皓二: Department of Chemistry, Faculty of Science, Kyoto University, Kyoto 606.

$\leq 1$ . These structures are easily understood by the following general principle. Metal atoms occupy octahedral holes of hexagonally close-packed chalcogen atoms. One end member  $MX$  with the NiAs-structure has only fully-occupied metal layers, while the other end member  $MX_2$  with the  $CdI_2$ -structure has the alternate stacking of fully-occupied and unoccupied metal layers (see Fig. 1). In the intermediate composition  $M_{1+y}X_2$  ( $0 < y < 1$ ), the unoccupied layers (van der Waals' gap) in the  $CdI_2$ -structure are partially occupied by the excess metal atoms  $y$ . Therefore, the layer stacking is generally  $M^fXM^vXM^fX\cdots$ , where  $M^f$  denotes the metal layer fully occupied and  $M^v$  the metal layer partially occupied. Moreover, metal-vacancies are characteristically arranged both within  $M^v$  layers and along the direction perpendicular to the layers at the specific composition.

Among these metal-vacancy-ordered phases,  $M_3X_4$  phase with the  $Cr_3S_4$ -structure\* (monoclinic) appears in many  $M_{1+y}X_2$  systems. Since this structure was first reported by Okazaki and Hirakawa in 1956,<sup>1)</sup> a number of isostructural compounds have been reported. The electric and magnetic properties of the compounds with the  $Cr_3S_4$ -structure are summarized in Table I. In the  $Cr_3S_4$ -structure,  $M^v$  layers are just half occupied and the metal-vacancies are arranged in such a manner as shown in Fig. 2. There exist two kinds of sites for metal atoms in this structure; the site I in  $M^v$  layers and the site II in  $M^f$  layers in the ratio 1:2.

On the basis of such a structural feature, many isostructural ternary compounds with the general formula  $M'M_2X_4$  have been also synthesized. Table II shows these compounds with their electric and magnetic properties. In these compounds, a metal-ordered structure is of interest. The type of the metal-ordered structure was first reported by Chevreton and Andron.<sup>2)</sup> They proposed the two cases on

Table I. Compounds with the  $Cr_3S_4$ -structure

Compound	Electric property <sup>a)</sup>	Magnetic property <sup>b)</sup>	References
$V_3S_4$	M	AF	12, 26, 41-47
$Cr_3S_4$	M	AF	12, 42, 48-51
$Ti_3Se_4$	M	PP	52
$V_3Se_4$	M	AF	26, 45, 52-56
$Cr_3Se_4$	SC	AF	27, 49, 50, 57-60, 100, 101, 104
$Fe_3Se_4$	SC	Fr	1, 61-64, 102, 103
$Co_3Se_4$	—	PP	15, 65, 66
$Ni_3Se_4$ <sup>c)</sup>	—	PP	32-34
$Ti_3Te_4$	—	PP	19, 30, 52
$V_3Te_4$	M	P	20, 28, 67-70
$Cr_3Te_4$	—	F(+AF)	19, 20, 49, 50, 60, 71-75, 99, 104

a) M: metallic, SC: semiconductive

b) P: paramagnetic, PP: Pauli paramagnetic, AF: antiferromagnetic, F: ferromagnetic, Fr: ferrimagnetic

c) The mixture with  $NiSe_2$ .

\* This structure is usually called as " $Cr_3S_4$ -structure" in spite of the first proposal for  $Fe_3Se_4$ .

Table II.  $M'M_2X_4$  with the  $Cr_3S_4$ -structure

## (a) Sulfides

Compound	Electric property <sup>a)</sup>	Magnetic property <sup>b)</sup>	References
FeTi <sub>2</sub> S <sub>4</sub>	M	AF + F, F	38, 39, 76–83, 105
CoTi <sub>2</sub> S <sub>4</sub>	M	PP	38–40, 81, 105
NiTi <sub>2</sub> S <sub>4</sub>	M	PP	38–40, 81, 105
CrV <sub>2</sub> S <sub>4</sub>	M, SC	AF	11, 12, 42
FeV <sub>2</sub> S <sub>4</sub>	M	AF	7–9, 40, 41, 79, 84, 85, 97
CoV <sub>2</sub> S <sub>4</sub>	M	PP	40, 41, 85
NiV <sub>2</sub> S <sub>4</sub>	M	PP	40, 41, 85, 86
TiCr <sub>2</sub> S <sub>4</sub>	M	AF	5, 41, 42
VCr <sub>2</sub> S <sub>4</sub>	SC	AF	10, 42
FeCr <sub>2</sub> S <sub>4</sub> <sup>c)</sup>	—	AF	87
CoCr <sub>2</sub> S <sub>4</sub> <sup>c)</sup>	—	AF	87
NiCr <sub>2</sub> S <sub>4</sub>	SC	AF + F	4, 35, 42, 48, 86, 87
TiFe <sub>2</sub> S <sub>4</sub>	SC	Fr	88
VFe <sub>2</sub> S <sub>4</sub>	—	AF	7, 9

## (b) Selenides

Compound	Electric property <sup>a)</sup>	Magnetic property <sup>b)</sup>	References
VTi <sub>2</sub> Se <sub>4</sub>	—	—	37
CrTi <sub>2</sub> Se <sub>4</sub>	—	—	30, 89
FeTi <sub>2</sub> Se <sub>4</sub>	M	AF	37–40, 79, 84
CoTi <sub>2</sub> Se <sub>4</sub>	M	PP	37–40
NiTi <sub>2</sub> Se <sub>4</sub>	M	PP	37–40
CrV <sub>2</sub> Se <sub>4</sub>	—	—	37
FeV <sub>2</sub> Se <sub>4</sub>	M	AF	37, 40, 79, 84, 90
CoV <sub>2</sub> Se <sub>4</sub>	—	PP	37, 40
NiV <sub>2</sub> Se <sub>4</sub>	M	PP	37, 40, 86, 91
TiCr <sub>2</sub> Se <sub>4</sub>	—	F	5, 30, 36
VCr <sub>2</sub> Se <sub>4</sub>	—	—	36
FeCr <sub>2</sub> Se <sub>4</sub>	SC	AF	2, 6, 16, 35, 36, 92, 96
CoCr <sub>2</sub> Se <sub>4</sub>	SC	AF	35, 36
NiCr <sub>2</sub> Se <sub>4</sub>	SC	AF	35, 36, 86
TiFe <sub>2</sub> Se <sub>4</sub>	SC	Fr	37, 93, 94
VFe <sub>2</sub> Se <sub>4</sub>	M	Fr	37, 93
CrFe <sub>2</sub> Se <sub>4</sub>	SC	Fr	16, 37, 93, 94
CoFe <sub>2</sub> Se <sub>4</sub>	M	Fr	15, 37, 93, 94
NiFe <sub>2</sub> Se <sub>4</sub>	M	Fr	15, 37, 93, 94
VCo <sub>2</sub> Se <sub>4</sub>	—	—	37
FeCo <sub>2</sub> Se <sub>4</sub>	—	P	15, 37
NiCo <sub>2</sub> Se <sub>4</sub>	—	—	37
FeNi <sub>2</sub> Se <sub>4</sub>	—	P	15, 37
CoNi <sub>2</sub> Se <sub>4</sub>	—	—	37

(c) Tellurides

Compound	Electric property <sup>a)</sup>	Magnetic property <sup>b)</sup>	References
VTi <sub>2</sub> Te <sub>4</sub>	—	—	95
CrTi <sub>2</sub> Te <sub>4</sub>	—	F	19, 30, 95
TiV <sub>2</sub> Te <sub>4</sub>	—	—	95
CrV <sub>2</sub> Te <sub>4</sub>	—	F	20, 95
FeV <sub>2</sub> Te <sub>4</sub>	M	AF	98
TiCr <sub>2</sub> Te <sub>4</sub>	—	F	3, 19, 95
VCr <sub>2</sub> Te <sub>4</sub>	—	F	20, 95

a) M: metallic, SC: semiconductive

b) AF: antiferromagnetic, F: ferromagnetic, Fr: ferrimagnetic, PP: Pauli paramagnetic

c) Synthesized under high pressure.

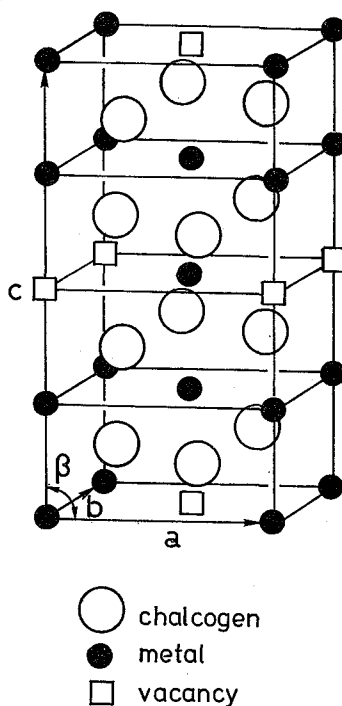


Fig. 2. Unit cell of the Cr<sub>3</sub>S<sub>4</sub>-structure

the analogy of those for the spinel compounds; (1) normal-type  $(M')[MM]X_4$ , (2) inverse-type  $(M)[M'M]X_4$ , where parentheses and brackets denote  $M^v$  and  $M^f$  layers, respectively. In fact, such metal-ordered structures have been found in several compounds mainly by neutron diffraction.<sup>2-7)</sup>

In addition to these binary or ternary compounds, some pseudo-binary systems  $M_3X_4$ - $M'_3X_4$  have also been studied mainly with a view to the electric and magnetic properties. The systems reported are as follows. (a) Sulfide system:  $V_3S_4$ -

$\text{FeV}_2\text{S}_4$ ,<sup>8)</sup>  $\text{V}_3\text{S}_4$ — $\text{VFe}_2\text{S}_4$ ,<sup>9)</sup>  $\text{Cr}_3\text{S}_4$ — $\text{V}_3\text{S}_4$ <sup>10-12)</sup> and  $\text{V}_3\text{S}_4$ — $\text{Ti}_3\text{S}_4$ .<sup>13,14)</sup> (b) Selenide system:  $\text{Ni}_3\text{Se}_4$ — $\text{Fe}_3\text{Se}_4$ ,<sup>15)</sup>  $\text{Co}_3\text{Se}_4$ — $\text{Fe}_3\text{Se}_4$ ,<sup>15)</sup> and  $\text{Cr}_3\text{Se}_4$ — $\text{Fe}_3\text{Se}_4$ .<sup>16)</sup> (c) Telluride system:  $\text{Cr}_3\text{Te}_4$ — $\text{Rh}_3\text{Te}_4$ ,<sup>17,18)</sup>  $\text{Cr}_3\text{Te}_4$ — $\text{Ti}_3\text{Te}_4$ ,<sup>19)</sup> and  $\text{Cr}_3\text{Te}_4$ — $\text{V}_3\text{Te}_4$ .<sup>20)</sup>

A study of the site preference of two kinds of metal ions in the pseudo-binary system  $\text{M}_3\text{X}_4$ — $\text{M}'_3\text{X}_4$  was for the first time made on the solid solution system  $\text{V}_3\text{S}_4$ — $\text{VFe}_2\text{S}_4$ .<sup>21)</sup> As a result, it was confirmed by neutron diffraction,<sup>7)</sup> Mössbauer spectroscopy,<sup>22)</sup> Raman spectroscopy<sup>23)</sup> and X-ray diffraction<sup>24)</sup> that Fe ions have a tendency for the site I in the  $\text{Cr}_3\text{S}_4$ -structure; Fe ions are preferentially substituted for V ions in the site I, starting from  $\text{V}_3\text{S}_4$ . The site preference of each metal ions was also observed in the system  $\text{TiS}_{1.40}$ — $\text{VS}_{1.40}$ .<sup>\*13)</sup> Results of the magnetic susceptibility and  $^{51}\text{V}$  NMR were successfully interpreted from the model that Ti ions preferentially occupy the site II. Nozaki also discussed the site preference in the Fe-V-S and Ti-V-S systems in relation to the interaction between cations along c-axis.<sup>25)</sup>

Another significant feature of  $\text{M}_3\text{X}_4$  phase is in the order-disorder transition of the metal-vacancies at higher temperatures. The following three transitions are possible, (1) the transition into the nonstoichiometric  $\text{CdI}_2$ -structure (intra-layer disordering of metal-vacancies), (2) the transition into the nonstoichiometric NiAs-structure (intra- and inter-layer disordering) and (3) the successive transition ( $\text{Cr}_3\text{S}_4$  →  $\text{CdI}_2$  → NiAs-structure). Oka *et al.* reported the transition of the type (1) in  $\text{V}_3\text{S}_4$  and  $\text{V}_3\text{Se}_4$ .<sup>26)</sup> The similar transition in  $\text{Cr}_3\text{Se}_4$  and  $\text{V}_3\text{Te}_4$  was reported by Ohtani *et al.*.<sup>27,28)</sup> Wada reported the transition of the type (3) in  $\text{Fe}_{0.60}\text{V}_{0.40}\text{S}_x$  ( $1.22 < x < 1.35$ ).<sup>29)</sup> The phase diagram of the system  $\text{M}_3\text{X}_4$ — $\text{M}'_3\text{X}_4$  in relation to the order-disorder transition of the metal-vacancies has been scarcely reported. We reported the phase diagram of  $(\text{Cr}_x\text{Ti}_{1-x})_3\text{Se}_4$ ,<sup>30)</sup> where the lattice parameters and the order-disorder transition temperature ( $T_c$ ) vs. composition curves were found to show an anomaly at the composition  $x=1/3$  ( $\text{CrTi}_2\text{Se}_4$ ). We interpreted the behavior from a viewpoint of the selective substitution of Cr ions for Ti ions in the site I and inferred the metal-ordered structure of  $\text{CrTi}_2\text{Se}_4$  and  $\text{TiCr}_2\text{Se}_4$  to be the normal- and inverse-type, respectively. Afterward, these metal-ordered structures were confirmed from the cation distribution in  $\text{CrTi}_2\text{Se}_4$  and  $\text{TiCr}_2\text{Se}_4$  determined by neutron diffraction.<sup>31)</sup>

Selenide systems are suitable in consideration of the site preference of each ion, because all of  $\text{M}_3\text{Se}_4$  (M: 3d-transition metal) except for  $\text{M}=\text{Mn}$  have the  $\text{Cr}_3\text{S}_4$ -structure. The establishment of the phase diagram of  $\text{M}_3\text{Se}_4$ — $\text{M}'_3\text{Se}_4$  system is indispensable also to understand their physical properties. In this paper, we report the phase diagrams of  $(\text{M}'_x\text{M}_{1-x})_3\text{Se}_4$  with all possible combinations (15 systems\*\*).

## EXPERIMENTAL

The samples were prepared by direct reaction of the high-purity elements.

\*  $\text{TiS}_{1.40}$  has  $4\text{H-Ti}_2\text{S}_3$ -type structure.

\*\* We excluded the  $(\text{Fe}_x\text{Ti}_{1-x})_3\text{Se}_4$  system because of some complexity. The phase diagram of the  $(\text{Fe}_x\text{Ti}_{1-x})_3\text{Se}_4$  system will be discussed in another paper.

Ti (3N), V (2N5), Cr (3N), Co (4N) and Ni (4N) were supplied in powder form. Fe powder was obtained from  $\text{Fe}_2\text{O}_3$  (4N) by reduction in  $\text{H}_2$ . Granular Se (5N) was ground into powder before use. They were mixed in the appropriate ratio, pressed into a disk at  $10 \text{ kg/cm}^2$  and sealed in an evacuated silica tube. The tube was then gradually heated up to  $800\text{--}900^\circ\text{C}$  and cooled to room temperature in an electric furnace. The products were pulverized and again pressed into a disk, followed by annealing at desired temperatures ( $300\text{--}900^\circ\text{C}$ ) and quenched in ice water. The annealing period was 1 week–1 month. The phase identification of the samples was made with an X-ray diffractometer with monochromatic  $\text{Cu K}\alpha$  radiation. The lattice parameters were determined by the least-squares method using the high-angle reflections.

X-ray diffraction patterns at high temperatures were taken with the X-ray diffractometer mounted with the furnace specially designed. The samples were sealed in an evacuated quartz capillary of 1–2 mm in diameter and 0.01 mm thick. To obtain sufficient diffraction intensity, three or four capillaries were mounted on a Pt plate.

Differential thermal analysis (DTA) was carried out in the temperature range from room temperature up to  $1100^\circ\text{C}$ . A heating or cooling rate was  $20\text{--}50^\circ\text{C/min}$ . The samples were sealed under vacuum in a cylindrical silica capsule with the thin-walled bottom (5 mm in diameter and 10 mm in height).  $\text{Al}_2\text{O}_3$ , Cr powder or blank capsule was used as references.

Electron diffraction patterns and lattice images were obtained with a JEM 100CX electron microscope.

## RESULTS AND DISCUSSION

### 1. Phase relation at room temperature

The samples quenched in ice water after annealing at various temperatures were identified at room temperature by X-ray powder diffraction. The results are as follows.

(a) The systems which form a solid solution with the  $\text{Cr}_3\text{S}_4$ -structure over a whole composition range;

$(\text{V}_x\text{Ti}_{1-x})_3\text{Se}_4$ ,  $(\text{Cr}_x\text{Ti}_{1-x})_3\text{Se}_4$ ,  $(\text{Cr}_x\text{V}_{1-x})_3\text{Se}_4$ ,  $(\text{Fe}_x\text{V}_{1-x})_3\text{Se}_4$ ,  $(\text{Co}_x\text{V}_{1-x})_3\text{Se}_4$ ,  $(\text{Fe}_x\text{Cr}_{1-x})_3\text{Se}_4$ ,  $(\text{Co}_x\text{Fe}_{1-x})_3\text{Se}_4$ ,  $(\text{Ni}_x\text{Fe}_{1-x})_3\text{Se}_4^*$  and  $(\text{Ni}_x\text{Co}_{1-x})_3\text{Se}_4^*$

(b) The systems in which two-phase mixture appeared;

$(\text{Co}_x\text{Ti}_{1-x})_3\text{Se}_4$ ,  $(\text{Ni}_x\text{Ti}_{1-x})_3\text{Se}_4^*$ ,  $(\text{Ni}_x\text{V}_{1-x})_3\text{Se}_4^*$ ,  $(\text{Co}_x\text{Cr}_{1-x})_3\text{Se}_4$  and  $(\text{Ni}_x\text{Cr}_{1-x})_3\text{Se}_4^*$

### 2. DTA

In all systems of the (a) group, one endothermic peak was observed in DTA. The peak temperature smoothly varies with the composition in these systems. Those

\* The stoichiometric  $\text{Ni}_3\text{Se}_4$  was the two-phase mixture of  $\text{M}_3\text{X}_4$  phase with the  $\text{Cr}_3\text{S}_4$ -structure and  $\text{NiSe}_2$  with the pyrite structure. This result agrees with the previous report on Ni-Se system.<sup>32–34</sup> Moreover, the pyrite phase appeared near  $\text{Ni}_3\text{Se}_4$  in the systems  $\text{M}_3\text{Se}_4\text{--Ni}_3\text{Se}_4$ . However, we omit the pyrite phase in the phase diagram shown later, because of a small amount of the phase.

of  $V_3Se_4$  and  $Cr_3Se_4$  are in good agreement with the order-disorder transition temperature ( $T_t$ ) reported by Oka *et al.*<sup>26)</sup> and by Ohtani *et al.*<sup>27)</sup> At higher temperatures, some samples showed several large endothermic peaks which probably correspond to an appearance of a liquid phase.

In the (b) group, the results of DTA were somewhat complex compared with those in the (a) group. In the solid solution region, one peak similar to that of the (a) group was observed, but two or three thermal anomalies were detected in the two phase region. As an example, the result of DTA in the  $(Co_xCr_{1-x})_3Se_4$  system is shown in Fig. 3. The result in the  $(Ni_xCr_{1-x})_3Se_4$  system was the similar one, but the DTA curves in the  $(Co_xTi_{1-x})_3Se_4$  and  $(Ni_xV_{1-x})_3Se_4$  systems did not show such definite peaks as those in the former two systems. In the  $(Ni_xTi_{1-x})_3Se_4$  system, no appreciable peak was observed except the endothermic peak at melting points (900–1000°C). In the present study, as is our interest focused mainly on the solid phase relation including the order-disorder transition, no further investigation about the liquid phase was performed.

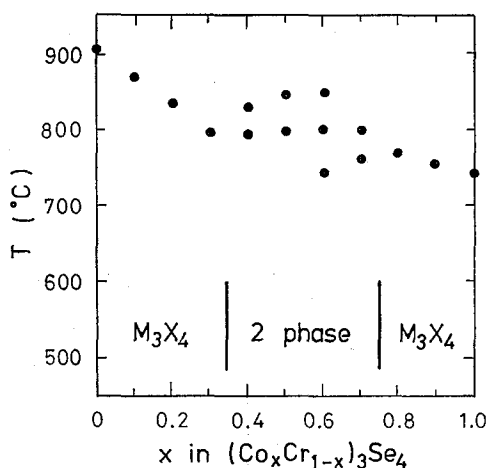


Fig. 3. Transition temperature detected by DTA in the  $(Co_xCr_{1-x})_3Se_4$  system

### 3. High-temperature X-ray diffraction

As is often the case with the transition metal chalcogenide,<sup>26,27,29)</sup> the high-temperature phases can be hardly quenched to room temperature. Therefore, the high-temperature X-ray diffraction experiments were carried out in several typical samples to clarify the high-temperature phase *in situ*.

#### 3.1 $Ni_3Se_4$

As mentioned before, nominal " $Ni_3Se_4$ " was  $M_3X_4$  phase with the  $Cr_3S_4$ -structure including a trace of  $NiSe_2$  with the pyrite structure. " $Ni_3Se_4$ " shows an endothermic peak in DTA at 370°C. Figure 4 shows the temperature dependence of a part of X-ray diffraction patterns characteristic of  $M_3X_4$  phase. The group of peaks at 300°C ( $M_3X_4$  phase) is gathering into a single peak on heating and finally



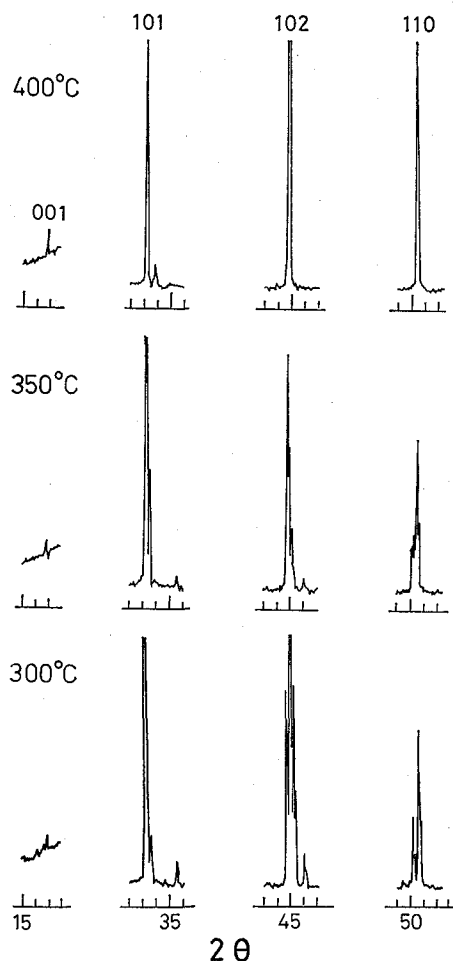


Fig. 4. A part of X-ray diffraction patterns of "Ni<sub>3</sub>Se<sub>4</sub>" observed at 300, 350 and 400°C. The indices hkl shown in the top of the figure are indexed on the CdI<sub>2</sub>-structure.

at 400°C the diffraction patterns completely show those of the CdI<sub>2</sub>-structure. The NiAs-structure as another possible high-temperature phase was excluded by the presence of 001 reflection at about  $2\theta = 17^\circ$ . Consequently, the transition at 370°C was confirmed to be the order-disorder transition from the Cr<sub>3</sub>S<sub>4</sub>- to CdI<sub>2</sub>-structure.

The high-temperature X-ray diffraction of Co<sub>3</sub>Se<sub>4</sub> also showed that the transition at 740°C accompanied with an endothermic peak is one from the Cr<sub>3</sub>S<sub>4</sub>- to CdI<sub>2</sub>-structure.

### 3.2 (Co<sub>0.6</sub>Cr<sub>0.4</sub>)<sub>3</sub>Se<sub>4</sub>

As shown in Fig. 3, (Co<sub>0.6</sub>Cr<sub>0.4</sub>)<sub>3</sub>Se<sub>4</sub> showed three endothermic peaks at 740, 800 and 850°C. The X-ray powder diffraction patterns of the sample show those of the mixture of two M<sub>3</sub>X<sub>4</sub> phases (Cr- and Co-rich M<sub>3</sub>X<sub>4</sub> phase) at room temperature. The results of the high-temperature X-ray diffraction patterns were

those of the mixture of two  $M_3X_4$  phases at 700°C,  $M_3X_4$  phase (Co-rich phase) and  $CdI_2$  phase (Cr-rich phase) at 775°C, two  $CdI_2$  phases at 820°C, and the single phase with the  $CdI_2$ -structure at 900°C. This reveals that two  $M_3X_4$  phases with the  $Cr_3S_4$ -structure separately exhibit the order-disorder transition at different temperature and form a solid solution with the  $CdI_2$ -structure at higher temperature. As seen in Fig. 3,  $T_t$  of each phase varies with composition  $x$  in the two phase region. The lattice parameters of each phase also varied in this region. This indicates that the tie-lines connecting the coexisting phases cross the binary line  $Cr_3Se_4$ — $Co_3Se_4$ , because  $Cr_3Se_4$  and  $Co_3Se_4$  phases have the wide nonstoichiometric region.

The similar successive phase transitions were also observed in the  $(Ni_xCr_{1-x})_3Se_4$  system.

#### 4. Phase diagram

From the results described in the preceding sections, we obtained following phase diagrams of the  $(M'_xM_{1-x})_3Se_4$  systems. The liquidus lines are omitted in the phase diagram shown below.

##### 4.1 $(Cr_xTi_{1-x})_3Se_4$

Figure 5 shows the phase diagram of the  $(Cr_xTi_{1-x})_3Se_4$  system.<sup>30)</sup> The  $T_t$  vs.  $x$  curve shows a minimum around  $x=1/3$  ( $CrTi_2Se_4$ ).

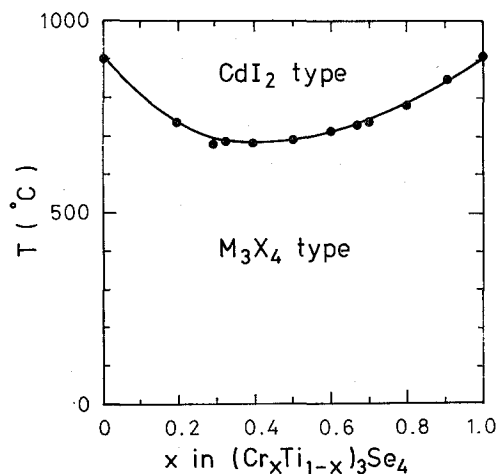


Fig. 5. Phase diagram of the  $(Cr_xTi_{1-x})_3Se_4$  system (from Ref. 30)

##### 4.2 $(Cr_xV_{1-x})_3Se_4$

This system also forms a solid solution with the  $Cr_3S_4$ -structure and exhibits the phase transition to the  $CdI_2$ -structure over a whole composition range. As shown in Fig. 6,  $T_t$  decreases monotonously as  $x$  increases, with slight downward curvature.

Phase Diagram of  $(M'_xM_{1-x})_3\text{Se}_4$  ( $0 \leq x \leq 1$ ); ( $M, M' = 3d\text{-transition metal}$ )

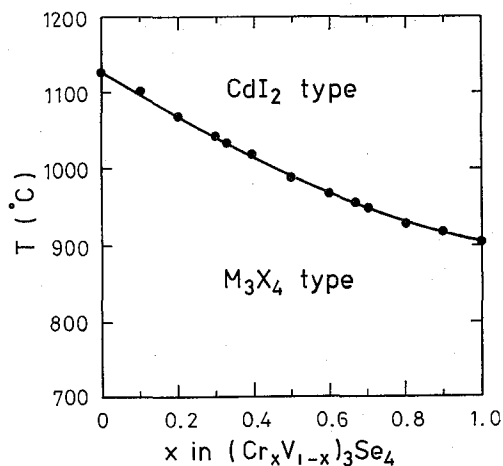


Fig. 6. Phase diagram of the  $(\text{Cr}_x\text{V}_{1-x})_3\text{Se}_4$  system

#### 4.3 $(\text{V}_x\text{Ti}_{1-x})_3\text{Se}_4$

The phase diagram of the  $(\text{V}_x\text{Ti}_{1-x})_3\text{Se}_4$  system is shown in Fig. 7. The  $T_t$  curve changes its curvature around  $x=2/3$  ( $\text{TiV}_2\text{Se}_4$ ).

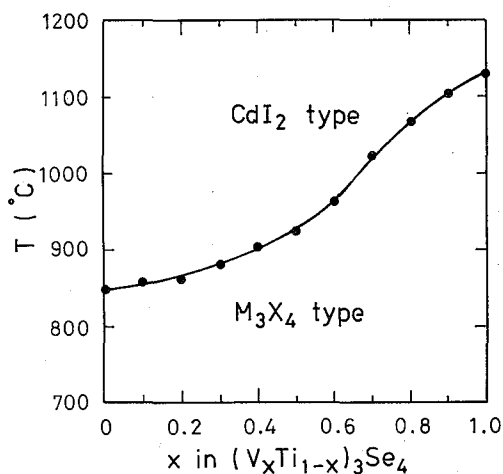


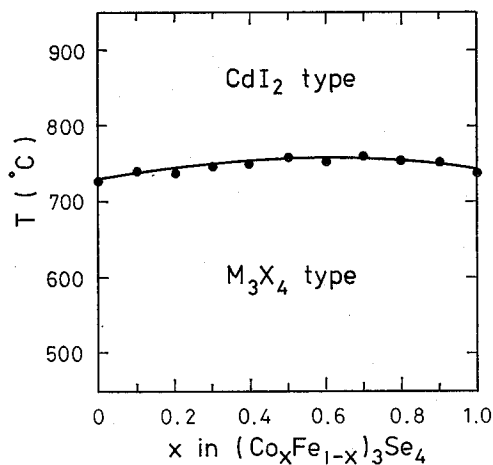
Fig. 7. Phase diagram of the  $(\text{V}_x\text{Ti}_{1-x})_3\text{Se}_4$  system

#### 4.4 $(\text{Co}_x\text{Fe}_{1-x})_3\text{Se}_4$

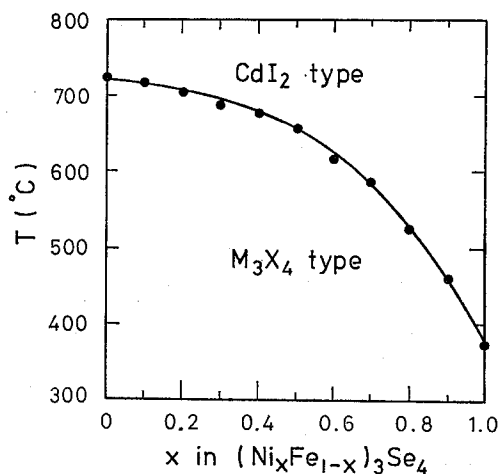
As shown in Fig. 8, this system forms a solid solution over a whole composition range, which agrees with the previous report.<sup>15)</sup> The  $T_t$  curve shows slight upward curvature.

#### 4.5 $(\text{Ni}_x\text{Fe}_{1-x})_3\text{Se}_4$

As mentioned before, when the samples were quenched from  $500^{\circ}\text{C}$ , a trace of the pyrite phase coexisted with  $\text{M}_3\text{X}_4$  phase in the composition range of  $0.8 \leq x$

Fig. 8. Phase diagram of the  $(\text{Co}_x\text{Fe}_{1-x})_3\text{Se}_4$  system

$\leq 1.0$ . This is consistent with the result reported by Kojima *et al.*<sup>15)</sup> However, we treat this system as a solid solution type. Figure 9 shows the phase diagram of the  $(\text{Ni}_x\text{Fe}_{1-x})_3\text{Se}_4$  system.  $T_t$  decreases with  $x$  and its curve shows upward curvature with no anomaly.

Fig. 9. Phase diagram of the  $(\text{Ni}_x\text{Fe}_{1-x})_3\text{Se}_4$  system

#### 4.6 $(\text{Ni}_x\text{Co}_{1-x})_3\text{Se}_4$

The pyrite phase also appears in this system. When the samples were quenched from 300 $^{\circ}\text{C}$ , the two phase region ( $\text{M}_3\text{X}_4$  phase + pyrite phase) was in the composition range of  $0.2 \leq x \leq 1.0$ . As an annealing temperature was raised, the two phase region became narrower ( $0.8 \leq x \leq 1.0$  for the samples quenched from 800 $^{\circ}\text{C}$ ). However, we treat this system as a solid solution type because of small amount of the

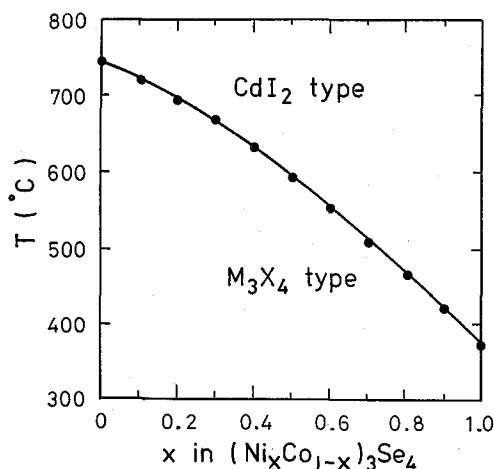


Fig. 10. Phase diagram of the  $(\text{Ni}_x\text{Co}_{1-x})_3\text{Se}_4$  system

pyrite phase. Figure 10 shows the phase diagram of the  $(\text{Ni}_x\text{Co}_{1-x})_3\text{Se}_4$  system.  $T_t$  smoothly decreases as  $x$  increases with slight upward curvature.

#### 4.7 $(\text{Fe}_x\text{V}_{1-x})_3\text{Se}_4$

Figure 11 shows the phase diagram of the  $(\text{Fe}_x\text{V}_{1-x})_3\text{Se}_4$  system. This system forms a solid solution over a whole composition range and  $T_t$  decreases monotonously with  $x$ . The  $T_t$  curve shows slight downward curvature.

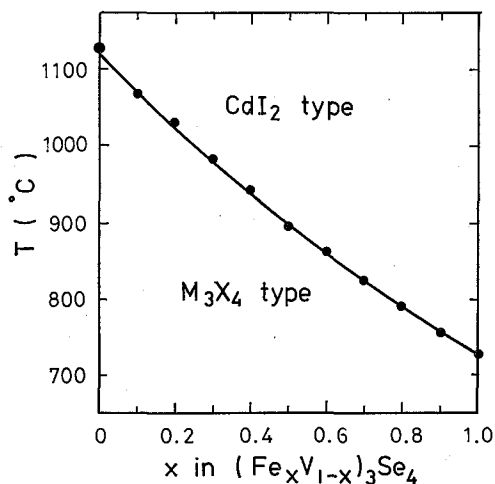
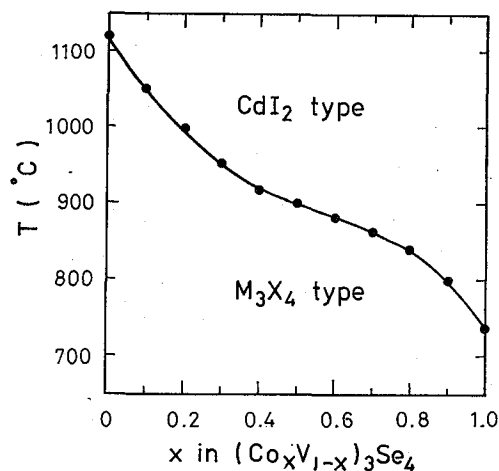


Fig. 11. Phase diagram of the  $(\text{Fe}_x\text{V}_{1-x})_3\text{Se}_4$  system

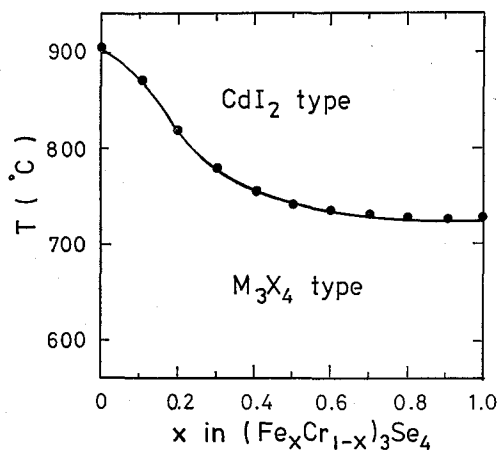
#### 4.8 $(\text{Co}_x\text{V}_{1-x})_3\text{Se}_4$

The phase diagram of the  $(\text{Co}_x\text{V}_{1-x})_3\text{Se}_4$  system is shown in Fig. 12.  $T_t$  decreases with  $x$  and the  $T_t$  curve shows a hump around  $x=2/3$  ( $\text{VCo}_2\text{Se}_4$ ).

Fig. 12. Phase diagram of the  $(\text{Co}_x\text{V}_{1-x})_3\text{Se}_4$  system

#### 4.9 $(\text{Fe}_x\text{Cr}_{1-x})_3\text{Se}_4$

This system forms a solid solution with the  $\text{Cr}_3\text{S}_4$ -structure over a whole composition range as shown in Fig. 13, which is in agreement with the previous report.<sup>16)</sup>  $T_t$  decreases steeply up to the composition about  $x=1/3$  ( $\text{FeCr}_2\text{Se}_4$ ), then decreases slightly toward  $x=1.0$ .

Fig. 13. Phase diagram of the  $(\text{Fe}_x\text{Cr}_{1-x})_3\text{Se}_4$  system

#### 4.10 $(\text{Co}_x\text{Cr}_{1-x})_3\text{Se}_4$

This system shows the phase separation as shown in Fig. 14. At low temperature, two phase region of Cr- and Co-rich  $\text{M}_3\text{X}_4$  phases was in  $0.3 \leq x \leq 0.8$ . As clarified by the high-temperature X-ray diffraction, each phase transformed into  $\text{CdI}_2$  phase at different temperatures. Then at higher temperature, a solid solution with the  $\text{CdI}_2$ -structure was formed in  $0 \leq x \leq 1$ . It is to be noted that " $\text{CoCr}_2\text{Se}_4$ " was the two phase mixture in this study, whereas the compound  $\text{CoCr}_2\text{Se}_4$  with

Phase Diagram of  $(M'_xM_{1-x})_3\text{Se}_4$  ( $0 \leq x \leq 1$ ); ( $M, M' = 3d\text{-transition metal}$ )

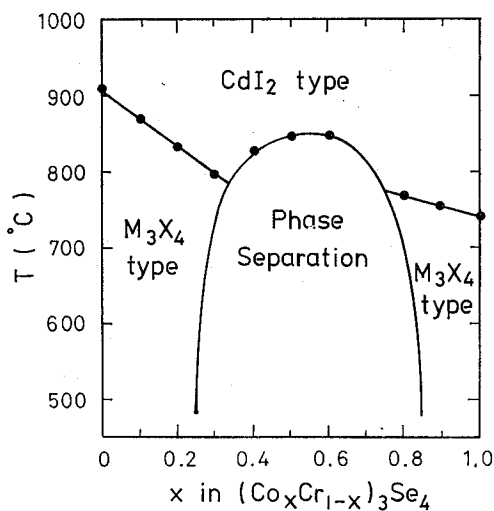


Fig. 14. Phase diagram of the  $(\text{Co}_x\text{Cr}_{1-x})_3\text{Se}_4$  system

the  $\text{Cr}_3\text{S}_4$ -structure was reported.<sup>35)</sup> Chevreton reported that “ $\text{CoCr}_2\text{Se}_4$ ” was not a single phase.<sup>36)</sup>

#### 4.11 $(\text{Ni}_x\text{Cr}_{1-x})_3\text{Se}_4$

Figure 15 shows the phase diagram of the  $(\text{Ni}_x\text{Cr}_{1-x})_3\text{Se}_4$  system. The obtained phase diagram is similar to that of the  $(\text{Co}_x\text{Cr}_{1-x})_3\text{Se}_4$  system.

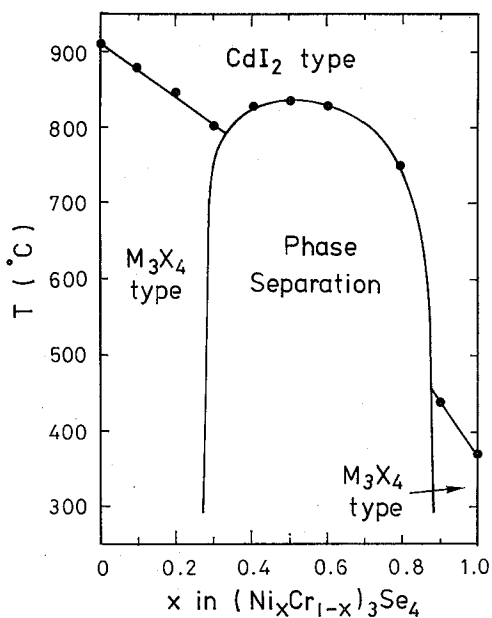
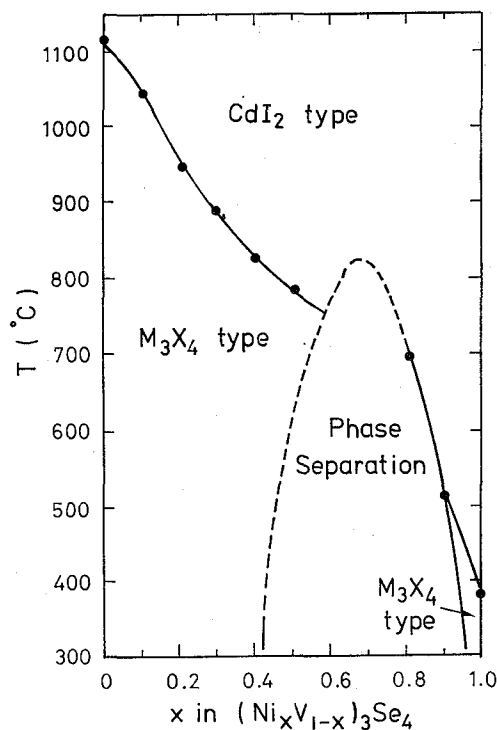


Fig. 15. Phase diagram of the  $(\text{Ni}_x\text{Cr}_{1-x})_3\text{Se}_4$  system

#### 4.12 $(\text{Ni}_x\text{V}_{1-x})_3\text{Se}_4$

We obtained the phase diagram shown in Fig. 16. Essentially, it resembles to

Fig. 16. Phase diagram of the  $(\text{Ni}_x\text{V}_{1-x})_3\text{Se}_4$  system

those of the former two systems, and the phase separation range was  $1/3 < x < 1$ .

#### 4.13 $(\text{Co}_x\text{Ti}_{1-x})_3\text{Se}_4$

In this system, the soluble region near  $\text{Co}_3\text{Se}_4$  was very narrow.  $\text{CdI}_2$  phase appeared in the composition range  $0.1 < x < 0.3$ .  $\text{M}_3\text{X}_4$  phase and  $\text{CdI}_2$  phase coexisted in the composition range  $0.3 < x < 1.0$  at low temperature. Figure 17 shows a tentative phase diagram of the  $(\text{Co}_x\text{Ti}_{1-x})_3\text{Se}_4$  system. Though the compound  $\text{CoTi}_2\text{Se}_4$  has been reported to have the  $\text{Cr}_3\text{S}_4$ -structure<sup>37,38</sup>, our result showed that it has the  $\text{CdI}_2$ -structure. This discrepancy seems to be caused by the thermal treatment.

#### 4.14 $(\text{Ni}_x\text{Ti}_{1-x})_3\text{Se}_4$

No distinct thermal anomaly was detected in DTA except ones owing to the appearance of liquid phase. The results of the phase identification of the samples annealed at various temperatures were as follows. As in the case of the  $(\text{Co}_x\text{Ti}_{1-x})_3\text{Se}_4$  system, the substitution of small amount of Ni for Ti suppresses  $\text{M}_3\text{X}_4$  phase. On the other hand, the soluble region near  $\text{Ni}_3\text{Se}_4$  was narrow. Figure 18 shows the temperature-product diagram. The phase transition to the  $\text{CdI}_2$ -structure around 67°C in  $\text{NiTi}_2\text{Se}_4$  reported by Plovnick *et al.*<sup>39</sup> was not detected in our DTA experiment.



Phase Diagram of  $(M'_xM_{1-x})_3\text{Se}_4$  ( $0 \leq x \leq 1$ ); ( $M, M' = 3d\text{-transition metal}$ )

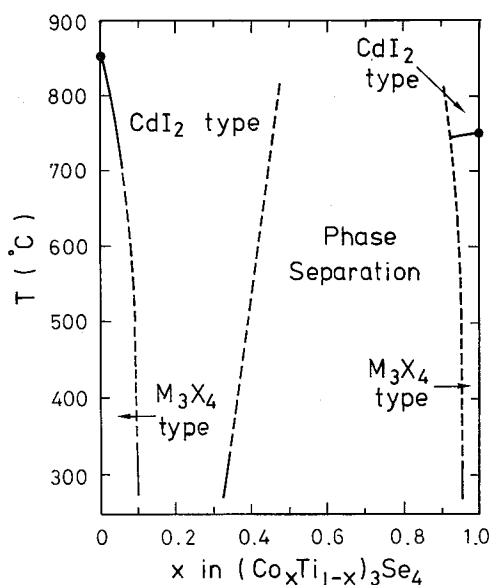


Fig. 17. Tentative phase diagram of the  $(\text{Co}_x\text{Ti}_{1-x})_3\text{Se}_4$  system

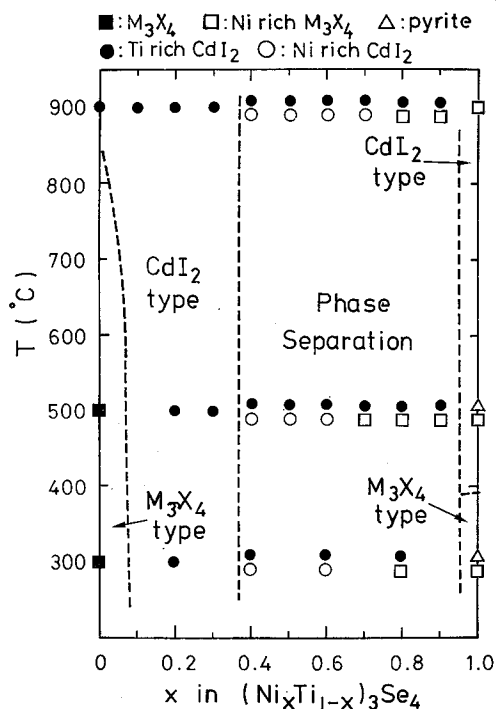


Fig. 18. Temperature-product diagram of the  $(\text{Ni}_x\text{Ti}_{1-x})_3\text{Se}_4$  system. Paired symbols denote two phase mixture.

### 5. Electron microscopic observation

As shown in the previous sections, some systems exhibit the phase separation at low temperature. To investigate the feature of the phase separation, the electron microscopy was performed. The sample was  $(\text{Co}_{0.6}\text{Cr}_{0.4})_3\text{Se}_4$  which was the mixture of two  $\text{M}_3\text{X}_4$  phases at room temperature as seen in Fig. 14. First, the sample was cooled rapidly from  $1050^\circ\text{C}$  which is far above the upper limit of the phase separation. The X-ray diffraction patterns, however, showed those of the mixture of two  $\text{M}_3\text{X}_4$  phases. A lattice image ([100] zone) of the sample is shown in Photo. 1. Dark and bright stripes with a width of about  $90\text{--}120\text{ \AA}$  are aligned alternately and each stripe consists of about 20 parallel lattice fringes. From the closer analysis of the electron diffraction patterns and lattice images, it was confirmed that the two  $\text{M}_3\text{X}_4$  phases with common a- and b-axis grow epitaxially along c-axis. The result of the X-ray diffraction in the  $(\text{Co}_x\text{Cr}_{1-x})_3\text{Se}_4$  system revealed that the dark and bright stripes correspond to Co- and Cr-rich  $\text{M}_3\text{X}_4$  phase, respectively. This indicates the feature of the phase separation by the anisotropic spinodal decomposition. Next, when the sample was reannealed in the phase separation region ( $800^\circ\text{C}$ ), it was perfectly separated into the two  $\text{M}_3\text{X}_4$  phases with no common axis and no stripe was observed in the electron microscopic photographs.

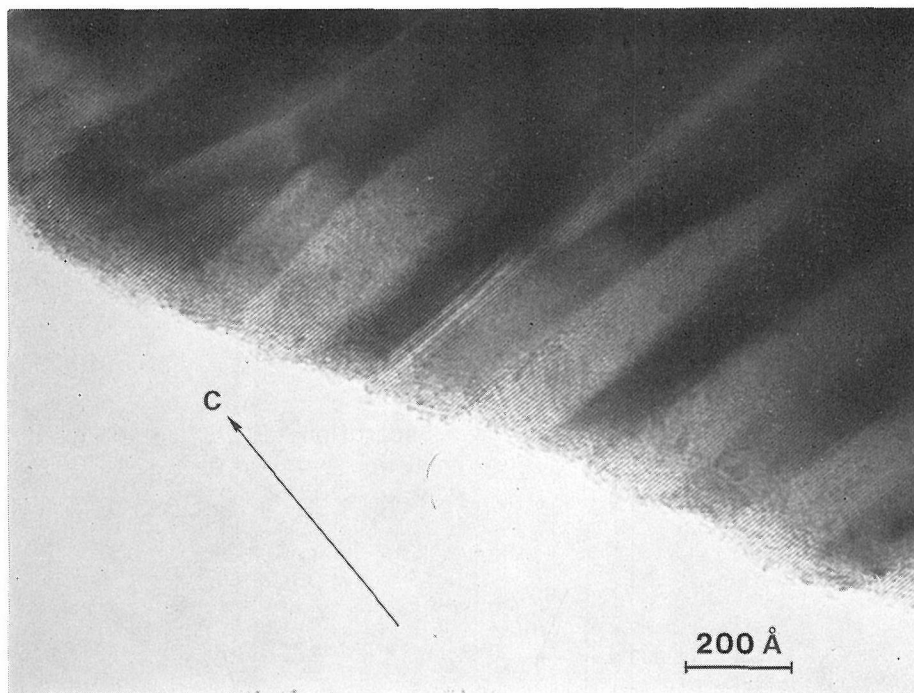


Photo. 1. Lattice image ([100] zone) of  $(\text{Co}_{0.6}\text{Cr}_{0.4})_3\text{Se}_4$  cooled rapidly from  $1050^\circ\text{C}$ . Dark and bright stripes correspond to Co- and Cr-rich  $\text{M}_3\text{X}_4$  phase, respectively (see text).

### CONCLUDING REMARKS

The obtained phase diagrams of the  $(\text{M}'_x\text{M}_{1-x})_3\text{Se}_4$  systems are classified into

Table III. Type of the phase diagram of the  $(M'_xM_{1-x})_3\text{Se}_4$  system

M'	M	Type <sup>a)</sup>
V	Ti	S.S.
Cr	Ti	S.S.
Co	Ti	P.S.
Ni	Ti	P.S.
Cr	V	S.S.
Fe	V	S.S.
Co	V	S.S.
Ni	V	P.S.
Fe	Cr	S.S.
Co	Cr	P.S.
Ni	Cr	P.S.
Co	Fe	S.S.
Ni	Fe	S.S.
Ni	Co	S.S.

a) S.S.: solid solution, P.S.: phase separation.

two types; solid solution type and phase separation type, as shown in Table III. The systems of any two of  $\text{Ti}_3\text{Se}_4$ ,  $\text{V}_3\text{Se}_4$  and  $\text{Cr}_3\text{Se}_4$ , and also any two of  $\text{Fe}_3\text{Se}_4$ ,  $\text{Co}_3\text{Se}_4$  and  $\text{Ni}_3\text{Se}_4$  form a solid solution and exhibit the phase transition from the  $\text{Cr}_3\text{S}_4$ - to  $\text{CdI}_2$ -structure over a whole composition range. On the other hand, several systems of the former three and the latter three show the phase separation.

An anomaly in the  $T_c$  curve was observed in several systems of solid solution type. This anomaly may be due to the site preference of each metal ion or the metal-ordered structure as confirmed in the  $(\text{Cr}_x\text{Ti}_{1-x})_3\text{Se}_4$  system<sup>30,31)</sup> and in  $\text{FeCr}_2\text{Se}_4$ .<sup>2,6)</sup>

The systems of phase separation type are subdivided according to the phase separation region. In the  $(\text{Co}_x\text{Cr}_{1-x})_3\text{Se}_4$  and  $(\text{Ni}_x\text{Cr}_{1-x})_3\text{Se}_4$  systems, the phase separation region spreads around the middle composition, while that in the  $(\text{Ni}_x\text{V}_{1-x})_3\text{Se}_4$ ,  $(\text{Co}_x\text{Ti}_{1-x})_3\text{Se}_4$  and  $(\text{Ni}_x\text{Ti}_{1-x})_3\text{Se}_4$  systems is in the composition range  $1/3 < x < 1$ . This suggests an intermediate compound at  $x=1/3$  in the latter case. A probable compound is the compound with the metal-ordered structure such as  $(\text{Ni})[\text{V}_2]\text{Se}_4$ ,  $(\text{Co})[\text{Ti}_2]\text{Se}_4$  and  $(\text{Ni})[\text{Ti}_2]\text{Se}_4$ . The determination of the metal-ordered structure by neutron diffraction, Mössbauer spectroscopy or NMR is now in progress.

#### ACKNOWLEDGMENTS

The authors wish to acknowledge the late professor S. Kachi for useful discussions in the early stage of this work. The authors are also grateful to K. Mochida, T. Nakai, S. Ohishi, H. Okamura, O. Okumura, T. Tanaka, T. Fujii, T. Kato and Y. Shimakawa for experimental assistance in the course of this study.

## REFERENCES

- ( 1 ) A. Okazaki and K. Hirakawa, *J. Phys. Soc. Jpn.* **11**, 930 (1956).
- ( 2 ) M. Chevreton and B. Andron, *C. R. Acad. Sci. Ser. B* **264**, 316 (1967).
- ( 3 ) B. Andron, G. Bérodiás, M. Chevreton and P. Mollard, *ibid.* **263**, 621 (1966).
- ( 4 ) B. Andron and E.F. Bertaut, *J. Phys. (Paris)* **27**, 619 (1966).
- ( 5 ) B. Lambert-Andron, G. Bérodiás and M. Chevreton, *Bull. Soc. fr. Minéral. Cristallogr.* **91**, 88 (1968).
- ( 6 ) K. Adachi, K. Sato and K. Kojima, *Mem. Fac. Eng. Nagoya Univ.* **22**, 253 (1970).
- ( 7 ) I. Kawada and H. Wada, *Physica* **105B**, 223 (1981).
- ( 8 ) Y. Oka, K. Kosuge and S. Kachi, *Mat. Res. Bull.* **12**, 1117 (1977).
- ( 9 ) H. Nozaki and H. Wada, *J. Solid State Chem.* **47**, 69 (1983).
- ( 10 ) Y. Tazuke, *Phys. Lett.* **69A**, 341 (1979).
- ( 11 ) Y. Tazuke, *Jpn. J. Appl. Phys.* **19**, Supplement 19-3, 367 (1980).
- ( 12 ) Y. Tazuke, *J. Phys. Soc. Jpn.* **50**, 413 (1981).
- ( 13 ) H. Nozaki, *Mat. Res. Bull.* **16**, 861 (1981).
- ( 14 ) Y. Tazuke, K. Watanabe and T. Suzuki, *J. Phys. Soc. Jpn.* **50**, 2900 (1981).
- ( 15 ) K. Kojima, S. Murase, K. Sato and K. Adachi, *J. Phys. Soc. Jpn.* **29**, 1642 (1970).
- ( 16 ) K. Kojima, M. Matsui, K. Sato and K. Adachi, *J. Phys. Soc. Jpn.* **29**, 1643 (1970).
- ( 17 ) A. Fujii, S. Ohta and S. Anzai, *Jpn. J. Appl. Phys.* **21**, 669 (1982).
- ( 18 ) S. Ohta, A. Fujii and S. Anzai, *J. Phys. Soc. Jpn.* **52**, 1765 (1983).
- ( 19 ) Y. Sugimoto, S. Ohta, S. Yuri, M. Tamaki and S. Anzai, *J. Phys. Soc. Jpn.* **54**, 3240 (1985).
- ( 20 ) S. Ohta, *J. Phys. Soc. Jpn.* **54**, 1076 (1985).
- ( 21 ) H. Wada, *Bull. Chem. Soc. Jpn.* **52**, 2130 (1979).
- ( 22 ) H. Nozaki, H. Wada and H. Yamamura, *Solid State Commun.* **44**, 63 (1982).
- ( 23 ) M. Ishii, H. Wada, H. Nozaki and I. Kawada, *Solid State Commun.* **42**, 605 (1982).
- ( 24 ) H. Nakazawa, K. Tsukimura, H. Hirai and H. Wada, *Acta Cryst.* **B39**, 532 (1983).
- ( 25 ) H. Nozaki, *J. Cryst. Soc. Jpn.* **26**, 220 (1984) [In Japanese].
- ( 26 ) Y. Oka, K. Kosuge and S. Kachi, *J. Solid State Chem.* **23**, 11 (1978).
- ( 27 ) T. Ohtani, R. Fujimoto, H. Yoshinaga, M. Nakahira and Y. Ueda, *J. Solid State Chem.* **48**, 161 (1983).
- ( 28 ) T. Ohtani, S. Onoue and M. Nakahira, *Mat. Res. Bull.* **19**, 1367 (1984).
- ( 29 ) H. Wada, *Bull. Chem. Soc. Jpn.* **52**, 2918 (1979).
- ( 30 ) Y. Ueda, K. Kosuge, M. Urabayashi, A. Hayashi, S. Kachi and S. Kawano, *J. Solid State Chem.* **56**, 263 (1985).
- ( 31 ) A. Hayashi, Y. Ueda, K. Kosuge, H. Murata, H. Asano, N. Watanabe and F. Izumi, (to be published).
- ( 32 ) F. Grønqvold and E. Jacobsen, *Acta Chem. Scand.* **10**, 1440 (1956).
- ( 33 ) J.E. Hiller and W. Wegener, *N. Jb. Miner., Abh.* **94**, 1147 (1960).
- ( 34 ) K.L. Komarek and K. Wessely, *Monatsh. Chem.* **103**, 923 (1972).
- ( 35 ) B.L. Morris, P. Russo and A. Wold, *J. Phys. Chem. Solids* **31**, 635 (1970).
- ( 36 ) M. Chevreton, *Acta Cryst.* **16**, A22 (1963).
- ( 37 ) G. Bérodiás and M. Chevreton, *C. R. Acad. Sci.* **261**, 2202 (1965).
- ( 38 ) R.H. Plovnick, M. Vlasse and A. Wold, *Inorg. Chem.* **7**, 127 (1968).
- ( 39 ) R.H. Plovnick, D.S. Perloff, M. Vlasse and A. Wold, *J. Phys. Chem. Solids* **29**, 1935 (1968).
- ( 40 ) B.L. Morris, R.H. Plovnick and A. Wold, *Solid State Commun.* **7**, 291 (1969).
- ( 41 ) M. Chevreton and A. Sapet, *C. R. Acad. Sci.* **261**, 928 (1965).
- ( 42 ) S.L. Holt, R.J. Bouchard and A. Wold, *J. Phys. Chem. Solids* **27**, 755 (1966).
- ( 43 ) A.B. De Vries and C. Haas, *J. Phys. Chem. Solids* **34**, 651 (1973).
- ( 44 ) I. Kawada, M. Nakano-Onoda, M. Ishii, M. Saeki and M. Nakahira, *J. Solid State Chem.* **15**, 246 (1975).
- ( 45 ) Y. Kitaoka, H. Yasuoka, Y. Oka, K. Kosuge and S. Kachi, *J. Phys. Soc. Jpn.* **46**, 1381 (1979).
- ( 46 ) Y. Kitaoka and H. Yasuoka, *J. Phys. Soc. Jpn.* **48**, 1949 (1980).
- ( 47 ) Y. Tazuke, T. Sato and Y. Miyako, *J. Phys. Soc. Jpn.* **51**, 2131 (1982).
- ( 48 ) F. Jellinek, *Acta Cryst.* **10**, 620 (1957).

- (49) E.F. Bertaut, G. Roult, R. Aleonard, R. Pauthenet, M. Chevreton and R. Jansen, *J. Phys. (Paris)* **25**, 582 (1964); *ibid.* **27**, 619 (1966).
- (50) D. Babot and M. Chevreton, *J. Solid State Chem.* **8**, 166 (1973).
- (51) H. Rau, *J. Less-Common Metals* **55**, 205 (1977).
- (52) M. Chevreton and F. Bertaut, *C.R. Acad. Sci. Ser. B* **255**, 1275 (1962).
- (53) E. Røst and L. Gjertsen, *Z. Anorg. Allg. Chem.* **328**, 299 (1964).
- (54) Y. Kitaoka and H. Yasuoka, *J. Phys. Soc. Jpn.* **48**, 1460 (1980).
- (55) K. Miyauchi, K. Hayashi and M. Nakahira, *Mat. Res. Bull.* **18**, 757 (1983).
- (56) A. Kallel and H. Boller, *J. Less-Common Metals* **102**, 213 (1984).
- (57) M. Chevreton and F. Bertaut, *C. R. Acad. Sci.* **253**, 145 (1961).
- (58) M. Chevreton, M. Murat, C. Eyraud and E.F. Bertaut, *J. Phys. (Paris)* **24**, 443 (1963).
- (59) M. Yuzuri, *J. Phys. Soc. Jpn.* **35**, 1252 (1973).
- (60) G. Peix, D. Babot and M. Chevreton, *J. Solid State Chem.* **36**, 161 (1981).
- (61) K. Hirakawa, *J. Phys. Soc. Jpn.* **12**, 929 (1957).
- (62) A.F. Andresen, *Acta Chem. Scand.* **22**, 827 (1968).
- (63) B. Lambert-Andron and G. Bérodiás, *Solid State Commun.* **7**, 623 (1969).
- (64) J.R. Regnard and J.C. Hocquenghem, *J. Phys. (Paris)* **32**, C1-268 (1971).
- (65) F. Bøhm, F. Grønvald, H. Haraldsen and H. Prydz, *Acta Chem. Scand.* **9**, 1510 (1955).
- (66) K.L. Komarek and K. Wessely, *Monatsh. Chem.* **103**, 896 (1972).
- (67) F. Grønvald, O. Hagberg and H. Haraldsen, *Acta Chem. Scand.* **12**, 971 (1958).
- (68) S. Brunie and M. Chevreton, *Bull. Soc. fr. Minéral. Cristallogr.* **91**, 422 (1968).
- (69) S. Anzai, S. Ohta, A. Yoshino, J. Nishio and M. Hatori, *Phys. Status Solidi* **B118**, K99 (1983).
- (70) T. Ohtani and H. Sakai, *Solid State Commun.* **57**, 81 (1986).
- (71) A.F. Andresen, *Acta Chem. Scand.* **24**, 3495 (1970).
- (72) K. Ozawa, S. Yanagisawa, T. Yoshimi, M. Ogawa and S. Anzai, *Phys. Status Solidi* **38**, 385 (1970).
- (73) J.M. Léger and J.P. Bastide, *Phys. Status Solidi* **A29**, 107 (1975).
- (74) M. Yamaguchi and T. Hashimoto, *J. Phys. Soc. Jpn.* **32**, 635 (1972).
- (75) H. Ipser, K.L. Komarek and K.O. Klepp, *J. Less-Common Metals* **92**, 265 (1983).
- (76) B.L. Morris, V. Johnson, R.H. Plovnick and A. Wold, *J. Appl. Phys.* **40**, 1299 (1969).
- (77) S. Muranaka, *Mat. Res. Bull.* **8**, 679 (1973).
- (78) S. Muranaka, *J. Phys. Soc. Jpn.* **35**, 616 (1973).
- (79) S. Muranaka and T. Takada, *Bull. Inst. Chem. Res., Kyoto Univ.* **51**, 287 (1973).
- (80) T. Takahashi and O. Yamada, *J. Solid State Chem.* **7**, 25 (1973).
- (81) M. Danot, J. Rouxel and O. Gorochoy, *Mat. Res. Bull.* **9**, 1383 (1974).
- (82) G.A. Fatséas, J.L. Dormann and M. Danot, *J. Phys. (Paris)* **40**, C2-367 (1979).
- (83) M. Katada and R.H. Herber, *J. Solid State Chem.* **33**, 361 (1980).
- (84) S. Muranaka and T. Takada, *J. Solid State Chem.* **14**, 291 (1975).
- (85) T. Murugesan, S. Ramesh, J. Gopalakrishnan and C.N.R. Rao, *J. Solid State Chem.* **44**, 119 (1982).
- (86) R.J. Bouchard and A. Wold, *J. Phys. Chem. Solids* **27**, 591 (1966).
- (87) R.E. Tressler and V.S. Stubican, *J. Am. Ceram. Soc.* **51**, 391 (1968).
- (88) S. Muranaka, *J. Phys. Soc. Jpn.* **35**, 1553 (1973).
- (89) N. Ohtsuka, K. Kosuge, N. Nakayama, Y. Ueda and S. Kachi, *J. Solid State Chem.* **45**, 411 (1982).
- (90) H.N. Ok and C.S. Lee, *Phys. Rev.* **B29**, 5168 (1984).
- (91) R.J. Bouchard, W.T. Robinson and A. Wold, *Inorg. Chem.* **5**, 977 (1966).
- (92) S.R. Hong and H.N. Ok, *Phys. Rev.* **B11**, 4176 (1975).
- (93) D. Babot, G. Bérodiás and B. Lambert-Andron, *J. Phys. (Paris)* **32**, C1-985 (1971).
- (94) J.R. Regnard and J. Chappert, *J. Phys. (Paris)* **34**, 721 (1973).
- (95) M. Chevreton and G. Bérodiás, *C. R. Acad. Sci.* **261**, 1251 (1965).
- (96) H.N. Ok and C.S. Lee, *Phys. Rev.* **B33**, 581 (1986).
- (97) Y. Oka, K. Kosuge and S. Kachi, *Mat. Res. Bull.* **15**, 521 (1980).
- (98) R.H. Plovnick, *J. Solid State Chem.* **5**, 153 (1972).
- (99) M. Chevreton, E.F. Bertaut and F. Jellinek, *Acta Cryst.* **16**, 431 (1963).

- (100) A. Maurer and G. Collin, *J. Solid State Chem.* **34**, 23 (1980).
- (101) D. Babot, M. Chevreton, J.L. Buevoz, R. Lagnier, B. Lambert-Andron and M. Wintenberger, *Solid State Commun.* **30**, 253 (1979).
- (102) F. Grønvald and E.F. Westrum, Jr., *Acta Chem. Scand.* **13**, 241 (1959).
- (103) F. Grønvald, *Acta Chem. Scand.* **22**, 1219 (1968).
- (104) M. Yuzuri and K. Segi, *Physica* **86-88B**, 891 (1977).
- (105) M. Inoue, M. Matsumoto, H. Negishi and H. Sakai, *J. Magn. Magn. Mat.* **53**, 131 (1985).